Volume 2, Issue 2, 2024 Copyright and License Grant: CC By 4.0



Synthesis of Nano-Biocomposite for Light-Weight Structural Applications

Nehemiah Mengistu Zeleke*¹, Devendra Kumar Sinha¹, Santosh Kumar² ¹Department of Mechanical Engineering, Adama Science and Technology University, Adama, Ethiopia

² School of Mechanical Engineering, Indian Institute of Technology, Varanasi, India *Corresponding Author's Email: Nehemiah.mengistu@gmail.com

Abstract

Biocomposite materials have brought additional possibilities to the manufacturing industry rather than synthetic materials. Biodegradable polymer materials such as Polylactide Acid (PLA) have attracted various industries for numerous applications due to their excellent properties such as tensile strength despite some weaknesses. However, their combination with varying weight percentages of Microcrystalline Cellulose (MCC) (0%, 3%, 6%, and 9%), Montmorillonite (MMT) nano clay (0%, 3%, 6%, and 9%) as reinforcing agents, and Sorbitol (S) (10%, 20%, 30%, and 40%) as plasticizers to enhance properties, fabricated at various temperatures (100°C, 125°C, 150°C, and 175°C) using the melt-mixing method, can be evaluated under different testing standards and optimized to achieve an optimal experimental setup. This study prepared 16 biocomposite samples through Taguchi's Orthogonal Array experimental design. The optimal factor level combination was investigated for Flexural Strength (FS) at 3% MCC and 9% MTT fillers, and 20% S plasticizer and at 175-degree centigrade, 3%MCC, 9%MTT, 20%S and 175-degree centigrade, at these levels, FS (Flexural Strength) is 96.5 MPa, Flexural Modulus (FM) (6%MCC, 9%MTT, 20%S, and 175-degree centigrade), at these control factors FM is 9.8 GPa, Tensile Strength (TS) (9%MCC, 9%MTT, 10%S, and 175-degree centigrade), at these levels, TS is 85.2 MPa, Young's Modulus (YM) (6%MCC, 9%MTT, 0%S, and 150-degree centigrade), at these experimental run YM is 4.22 GPa, Water Absorption (WA) (0% MCC, 0% MTT, 0% S and 150 degree centigrade), WA is 2.42% and Density (D) (9%MCC, 9%MTT, 30%S and 175 degree centigrade) at this experimental setup D is 0.0427g/mm3. A general multiple linear model was established for each result prediction. Analysis of variance (ANOVA) for the regression model shows the statistical significance of the regression model and the significance of the factors that affect each response. The addition of fillers and plasticizers significantly improves the properties of PLA material and the developed biocomposite material is expected to be utilized for lightweight load-carrying applications in structural and biomedical areas.

Keywords: Biocomposite, Micro Crystalline Cellulose, Montmorillonite, Polylactide Acid, Sorbitol, Multiple Linear Model

Received: July 2024; Revised: 29 November 2024; Accepted: 15 December 2024; Published: 23 December 2024

(P): 2959-393X **DOI:** https://doi.org/10.59122/174CFC14

Copyright and License Grant: CC By 4.0



I. Introduction

Material designers and processing firms are in unwavering investigation for novel and enhanced materials and fabrication methods to make materials that have enhanced mechanical properties, that are renewable, eco-friendly, and of low cost. One of the areas that gained the most attention in this regard is the field of biocomposite also alternatively referred to as natural fiber composite [1]. Biocomposite is a combined constituent made from natural resources as a strengthening and the matrix is produced by a polymer from synthetic or natural materials [2]. This biocomposite material has numerous advantages in terms of its ecofriendliness, recyclability, biodegradability, low density, carbon dioxide neutrality (non-toxic), good insulating and acoustic properties, good thermal properties, and non-abrasiveness [3-5]. As a result, it has many industrial applications in the fields of automotive, building, packaging, and furniture [6]. Natural fibers contain three main essential polymers: hemicellulose and cellulose are the polysaccharides and those called holocellulose and lignin are the aromatic polymers. The lignin and hemicellulose content in fibers influences the end characteristics of biocomposites as they have a higher attraction for moisture and are hydrophilic. Researchers and material engineers have devoted themselves to the elimination of these (hemicellulose and lignin) contents in cellulose applications and their derivatives microcrystalline cellulose (MCC) and Nano-cellulose (NC) as fillers in different polymers. Additionally, they are in continuous search for new and higher sources of cellulose material and high amounts of cellulose-based biocomposite materials [7]. Cellulose is the abundant and most essential polymer in nature, which can be derived from renewable resources. Its presence as the common constituent on the cell wall of plants was first observed by Braconnot in 1819 [8]. It has a dense microfibril structure with a linear chain of β -1,4-glycosidic-linked D-glucose units as the main building blocks having crystallinity and strong hydrogen bonds that offer excellent mechanical strength, nontoxic, and biodegradability properties [9]. It is a promising renewable and biodegradable resource that could potentially substitute man-made fibers in industrial applications [10]. It is extensively utilized in numerous areas, such as water treatment, food industry packaging, biomaterial composites, textile and paper manufacturing, and the pharmaceutical industry as a raw material [11]. Numerous plants such as jute, flax, hemp, bamboo, wood, and cotton have abundant cellulose content [12]. Furthermore, cellulose has been isolated from different resources, i.e. hop stems [13], milkweed stems [14], coffee husks [15], rice husks [16], Cissus quadrangularis root [17], etc.Its derivative, microcrystalline cellulose, is a tasteless and micro-sized naturally available constituent investigated from partially depolymerized and purified cellulose. Cellulose chains are combined to make microfibrils and these microfibrils are additionally combined to make "cellulose macro fibers". Therefore, natural fibers that hold cellulose structure are considered "cellulose microfibers", which contain both "amorphous" and

Volume 2, Issue 2, 2024

DOI: https://doi.org/10.59122/174CFC14



Copyright and License Grant: CC By 4.0



"crystalline" cellulose regions [18]. Acidic attack treatment is used to reduce cellulose macro fibers properties by removing the amorphous region for the intention of crystalline region separation. Then, these crystallites can move without restrictions due to an increase in size. In research works, this structure is generally named "microcrystalline cellulose". Its extraction techniques are various containing biological, chemical, and mechanical treatment. Chemical treatment, predominantly acid hydrolysis, is the common technique used for the isolation of MCC [19]. Polylactic acid is a bio-degradable and eco-friendly polymer made up of lactic acid by-products such as starch sugar cane, potatoes, corn grain, etc., and renewable agricultural products [20, 21]. It is considered a leading candidate thermoplastic polymer that yields different components for structural, packaging, and biocompatibility applications. Currently, different biobased polymer materials are used for binding natural fibers. Among these polymers, PLA is the dominant one that is being studied intensively [22]. However, it has low performance on mechanical and thermal properties as well as high cost. These pose great scientific challenges and limit their large-scale applications to outdoor environments [23, 24]. Recently, several studies that used plasticization [25], copolymerization [26], blending [27], fiber-reinforced composite [28], and nano-based composite [29] fabrication have been done to enhance the PLA bioplastic properties. Plasticizers are commonly used materials to modify polymers and are considered the most common plastic material additive. They are a type of non-volatile and low molecular weight organic compounds that improve the processability and flexibility of the polymer by decreasing the glass transition temperature. The plasticizing theory assumes that the low molecular weight of a plasticizer permits decreasing connecting forces such as Vander Waals forces, hydrogen bonding, etc. between the polymer chains by penetrating the intermolecular spaces and reducing the intermolecular frictions [30]. The inclusion of these materials in polymers influences the viscosity, density, elastic modulus, hardness, impact resistance, water absorption, crystallization, melting temperatures, permeability, and degradation rate [31]. Plasticizers can be differentiated into petro-based or bio-based. Bio-based plasticizers are assumed as ideal green plasticizers and non-toxic, have good miscibility, are efficient, low cost, high resistance to leach from polymer. The most common bio-based plasticizers are polyols such as glycerol, diethylene glycol, ethylene glycol, tri ethylene glycol, tetra ethylene glycol propylene glycol, polyethylene glycol, xylitol, mannitol and sorbitol, monosaccharides (glucose, fructose, mannose, sucrose), fatty acids, vegetable oils, ethanolamine, urea, triethanolamine, lecithin, waxes, surfactants, amino acids, and water [32]. The inclusion of a plasticizer in biodegradable composites reduces the composite fragility behavior noticeably [33]. As a plasticizer, sorbitol has superior mechanical and physicochemical properties than other polyols [34]. As the study reports, the incorporation of sorbitol plasticizer amounts up to 30 wt.%, simplifies the creation of crystalline areas in chitosan films. These

Volume 2, Issue 2, 2024

DOI: https://doi.org/10.59122/174CFC14



Copyright and License Grant: CC By 4.0



crystalline areas act as cross-links limiting the movement of amorphous chemical chains and lead to improvement in thermo gravimetric results. Furthermore, the inclusion of sorbitol was capable to increase the physicochemical and thermal characteristics of chitosan films [35].

Clay is a material class having layered clay minerals or silicates with traces of organic matter and metal oxides. The classes of clays are classified in terms of their crystal structure and chemical compositions. Based on the ratios of its building block (silica tetrahedron and aluminum (or other) octahedron) natural clay is categorized into three groups kaolinite (1:1), montmorillonite, and vermiculite (2:1) and chlorite (2:2), related with constitutive interchanging layers of "SiO2" and "AlO6" units. Montmorillonite (MMT) is the frequently used Nano clay because of its availability, eco-friendliness, high aspect ratio, high swelling property in polar spaces, and well-analyzed chemistry [36, 37]. The incorporation of Nano clay into polymers and natural fiber-reinforced polymers improves the performance (physical, mechanical, thermal, ultraviolet, diffusional barrier, etc.) of Nanocomposites [38]. The mechanical property of polymer matrix composite is greatly enhanced due to the interfacial level interaction between the constituent and better dispersion of the Nano clay in the polymer matrix. This ensures better load transfer between them and highly uniform stress distribution for better properties [39]. Previously, conducted research work has shown Nano clay's usefulness to make excellent properties of biocomposites. Nano clay content addition is considered a basic constituent. The inclusion of Nano clay into a polyester matrix improves the mechanical performance and decreases the shrinkage of the composite material [40]. On the same matrix material incorporation of graded Nano clay, the flexural and tensile strength with modulus improves [41]. Additionally, the loading of Nano clay, Nanomer I30 E, into epoxy resin enhanced the tensile strength with a reduction in strain at failure [42]. The addition of Cloisite 20A Nano clay enhanced the mechanical properties of vinyl ester composites, specifically fracture toughness with an insignificant reduction in flexural strength [43]. Moreover, it has been verified that the flammability behavior of polymer composite is improved with a charging of 2 % of Nano clay [44].

Optimization is an important method used to determine the well-known design factors that can provide the optimal (maximum or minimum) result for a given problem. Problems of optimization are figured out through non-conventional and conventional techniques [45]. Non-conventional optimization techniques were used for the optimization of multi-response characteristics. Conventional techniques are statistical designs of experiments that consist of response surface methodology and Taguchi's method. These methods were used to find the optimal factors of single-quality characteristics. Taguchi's method has a special design method called an orthogonal array used to analyze a large number of factors with a lesser number of experiments. The results drawn from these small experiments are acceptable over the whole experimental

Volume 2, Issue 2, 2024

DOI: https://doi.org/10.59122/174CFC14



Copyright and License Grant: CC By 4.0



domain varied by the control factor and its levels. The result of experiments is converted into a signal-to-noise (S/N) ratio. It is used to measure the deviation of the response from the desired value.

Based on this background, in the present study, the flexural strength, flexural modulus, tensile strength, Young modulus, hardness, water absorption, and density properties of PLA-based biocomposite at different filler (MCC and MTT) and plasticizing (sorbitol) content with operating parameter (temperature) are determined. Fillers and plasticizer content with operating parameters are considered as process parameters to determine how they behave for flexural stress, tensile stress, and indentation. Taguchi's orthogonal array is used to optimize the responses of PLA-based developed biocomposite. Regression model analysis of variance is executed to expose the statistical significance of the regression model and the significance factor level of influence on the responses of developed biocomposite.

II. Materials and Methods

A. Description of Materials and Bio-composite Preparation

In this study, the biocomposite sample material used is made from coffee husk-derived MCC and MMT Nano clay powder as a reinforcing agent, and PLA as a matrix material. Additionally, sorbitol powder was used as a plasticizer. The PLA grade NCZ-NP-381/22, MMT Nano clay grade NCZ-MN-118/20, and D-sorbitol were supplied from India, Aritech Chemazone Pvt. Ltd. The reinforcing material, MCC was extracted from the outer skin of isolated coffee husk according to the procedure reported in Nehemiah M.Z et.al [15]. All samples of MCC/MMT/S/PLA biocomposite were fabricated using the melt-mixing method. Initially, the designated weight percentage of PLA and sorbitol were mixed and heated at the required temperature on the heating plate. Then, pre-calculated amounts of MCC and MMT were added to the heated blend of PLA and sorbitol and stirred properly to make uniform distributions of reinforcing agent. After that, the material was poured into the mold size of 100x50x4mm with a constant pressure of 2 MPa for 24 hrs. It was then cut into the specimens using a hacksaw according to ASTM standards and sanded using sandpaper. Finally, the post-curing of specimens was carried out at 40 °C temperature in an oven for 3 hours to remove the existence of moisture that may affect the final results.

B. Experimental Design and Plan of Investigation

In the present research investigation, biocomposite material based on Polylactide acid with coffee husk-derived MCC and MTT particles, and an S plasticizer at different T was prepared using a melt mixing setup. The intended amount of MCC and MMT particles were mixed properly to make homogeneous distributions. For the preparation of biocomposite material, four effective parameters (MCC, MTT, S, and T) with four levels for each parameter were used to investigate responses. The control factors and their levels are





exhibited in Table I below. The response factors tensile strength and modulus, flexural strength and modulus, hardness value, water absorption, and density values were measured according to their respective ASTM standards.

Table I: Control factors and their values at four levels

Factors	TIm:4	Levels			
Factors	Unit	1	2	3	4
A – MCC	Wt. %	0	3	6	9
B – MMT Nano clay	Wt. %	0	3	6	9
C – Sorbitol	Wt. %	0	10	20	30
D – Temperature	°C	100	125	150	175

Taguchi's method has a special design method called orthogonal array used to analyze a large number of factors with a lesser number of experiments. The results drawn from these small experiments are acceptable over the whole experimental domain varied by the control factor and its levels. The result of experiments is changed into a signal-to-noise ratio. It helps to evaluate the variation of the response from the preferred value. Based on the type of desired response, S/N ratio analysis is categorized into three, i.e. the higher the better, the lower the better, and the nominal the better. For developed biocomposite, flexural strength, tensile strength, hardness value, and density have been thought of as the larger-the-better; and for water absorption, it is the smaller-the-better. The S/N ratio for the corresponding responses was calculated using the following cases.

Case 1: The larger-the-better performance characteristics are utilized for a problem when maximization of interest is required.

$$S/N \ ratio = -10 \ log_{10} \left(\frac{1}{n}\right) \sum_{i=1}^{n} \frac{1}{y_{ij}^2}$$
 (1)

Where: y_{ij} - observed response value, n - Number of replications, i=1, 2, ...n; j=1, 2, ...k

Case 2: The smaller-the-better performance characteristics are used for a problem where minimization of interest is required.

$$S/N \ ratio = -10 \ log_{10} \left(\frac{1}{n}\right) \sum_{i=1}^{n} y_{ij}^{2}$$
 (2)

Taguchi's orthogonal array (L16) experimental design made by "Minitab" software is shown in Table II.

(D)

(P): 2959-393X

DOI: https://doi.org/10.59122/174CFC14

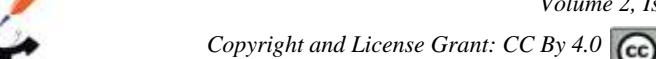


Table II: L16-OA design matrix for biocomposite development

Sample	Coded Factor				Uncoded Factor			
No.	A	В	С	D	MCC (Wt. %)	MMT (Wt. %)	S (Wt. %)	T (0C)
1	1	1	1	1	0	0	10	100
2	1	2	2	2	0	3	20	125
3	1	3	3	3	0	6	30	150
4	1	4	4	4	0	9	40	175
5	2	1	2	3	3	0	20	150
6	2	2	1	4	3	3	10	175
7	2	3	4	1	3	6	40	100
8	2	4	3	2	3	9	30	125
9	3	1	3	4	6	0	30	175
10	3	2	4	3	6	3	40	150
11	3	3	1	2	6	6	10	125
12	3	4	2	1	6	9	20	100
13	4	1	4	2	9	0	40	125
14	4	2	3	1	9	3	30	100
15	4	3	2	4	9	6	20	175
16	4	4	1	3	9	9	10	150

C. Regression analysis

The factors (MCC, MTT, S, and T) were considered in the development of mathematical models for the response value (TS, YM, FS, FM, HV, WA, and D) accuracy. The correlation between factors (MCC, MTT, S, and T) and response values (TS, YM, FS, FM, HV, WA, and D) accuracy of developed biocomposite was obtained by multiple linear regression, which is a technique that analyzes numerous explanatory factors to forecast the result of performance characteristics [46]. A linear model is developed to control the response (TS, YM, FS, FM, HV, WA, and D) data fitness to represent a characteristic in the form as follows:

$$Y = b_0 + b_1 MCC + b_2 MTT + b_3 S + b_4 T + \varepsilon$$
 (3)

Where Y is the response, b_1 , b_2 , b_3 , and b_4 are estimates of the factors and ε is the error. The statistical software package MINITAB was applied to develop the models.

D. Characterization Techniques of Developed Biocomposite

1) Flexural: The flexural strength of the samples was determined as per ASTM D790 through-point bend testing method by UTM machine, i.e. Bongshin Model DSCK machine [47, 48]. The flexural strength and modulus were determined with the given equations;

Copyright and License Grant: CC By 4.0



Flexural strength, FS = $\frac{3FL}{2wt^2}$ (4)

Flexural modulus, FM =
$$\frac{L^3 F}{4wt^3 \delta}$$
 (5)

Where F - is the applied load, L - is the length of the specimen, w - is the width of the specimen, t - is the thickness of the specimen and δ - is the deflection.

- 2) *Tensile:* tensile was performed based on ASTM D638 to measure the tensile strength of the samples [49][50].
- 3) Water absorption: the material's water absorption is important to study in case the developed materials are used in contact with water for determining water uptake in contact with water. This can adversely affect mechanical and ageing properties. The investigation was conducted according to ASTM D570-98, sample size of 20x20x3mm to find out the water absorption of specimens [51]. The water absorption of the specimens was determined as an increase in weight % with the following equation [52].

Increase in weight % = (wet weight – dry weight)/dry weight x 100 (6)

4) *Density:* the density of developed biocomposite specimens was carried out according to ASTMD792-98, sample size of 20x20x3mm. Then, the density was determined through the given equation [53].

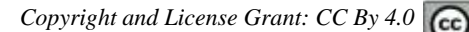
Density = Mass (g)/Volume (mm
3
) (7)

III. Results and Discussion

A. Flexural Strength and Modulus of Biocomposite

The flexural strength and modulus of biocomposite samples at different weight percentage of MCC, MTT, and S in PLA at various temperature levels are shown in Table III with their S/N ratio and Fig. 2. Under flexural loading, Table II and Fig. 2 exhibit that the addition of MCC, MTT and S improved the flexural strength and modulus of neat PLA. The flexural strength values of the MCC and MTT reinforced and S plasticized PLA (MCC/MTT/S/PLA) biocomposites could be higher than the neat PLA except for 9MCC/0MTT/30S/125T values at experiment 13. This is probably due to the establishment of agglomeration at higher content of MCC and because increasing S content at higher levels leads to low flexural strength due to its low flexural strength [54]. The experimental setup 3MCC/9MTT/20S/125T combination shows the highest flexural strength with the value of 93.75 MPa as shown in experiment 8, which is 78.5 % greater than that of the neat PLA experiment 1. It is easily assumed that at these contents the fillers are dispersed uniformly within the PLA material. It is clearly shown in Table III that the flexural modulus of each MCC/MTT/S bio-composite sample is greater than that of the neat PLA. This is mainly

DOI: https://doi.org/10.59122/174CFC14





caused due to flexural 3-point bending tests in which the upper half part of the cross-section of the sample is in compression, whereas the lower half part of the cross-section is subjected to tensile loads. Therefore, the parting boundary would be hindered in the sample on the side compressive, resulting in an improved load transfer mechanism from the matrix material to the fillers [55].

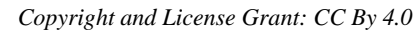
Table III: Flexural strength and modulus of biocomposite with s/n ratios

S. N		Facto	ors		Responses			
5. IN	MCC	MMT	S	T	FS (MPa)	S/N Ratio	FM (GPa)	S/N Ratio
1	0	0	0	100	52.50	34.40	4.1	72.19
2	0	3	10	125	60.00	35.56	5.3	74.53
3	0	6	20	150	75.00	37.50	6.7	76.59
4	0	9	30	175	82.50	38.32	7.5	77.54
5	3	0	10	150	60.00	35.56	5.5	74.89
6	3	3	0	175	71.25	37.05	7.1	77.01
7	3	6	30	100	75.00	37.50	7.5	77.58
8	3	9	20	125	93.75	39.43	9.7	79.79
9	6	0	20	175	63.75	36.08	6.7	76.58
10	6	3	30	150	63.75	36.08	7.1	77.00
11	6	6	0	125	67.50	36.58	7.7	77.79
12	6	9	10	100	71.25	37.05	8.4	78.57
13	9	0	30	125	45.00	33.06	5.0	73.97
14	9	3	20	100	56.25	35.00	8.1	78.22
15	9	6	10	175	56.25	35.00	7.8	77.85
16	9	9	0	150	60.00	35.56	8.6	78.78

The best S/N ratio shown in Table III for FS is 39.43 at experiment number 8 and also offers a higher FS value of 93.75. The weakest S/N ratio is 33.06 observed in experiment 13. The best S/N ratio of FM is observed in the same experimental setup, experiment 8 with a value of 79.79, and the weakest S/N ratio is observed in experiment 1 with a value of 72.19.

B. Probability Plot

Fig. 1 presents the probability plot of flexural strength and modulus of all samples. As exhibited in Fig. 1 (a) and (b) all data are under normal distribution at the confidence level of 95%. The two lines beside the center line on the left and right show the upper and lower limits of the confidence interval. No sample value is out of the confidence interval. Additionally, the p-values 0.657 and 0.544, which are higher than the significance level of 0.05 show that the data follows a normal distribution.







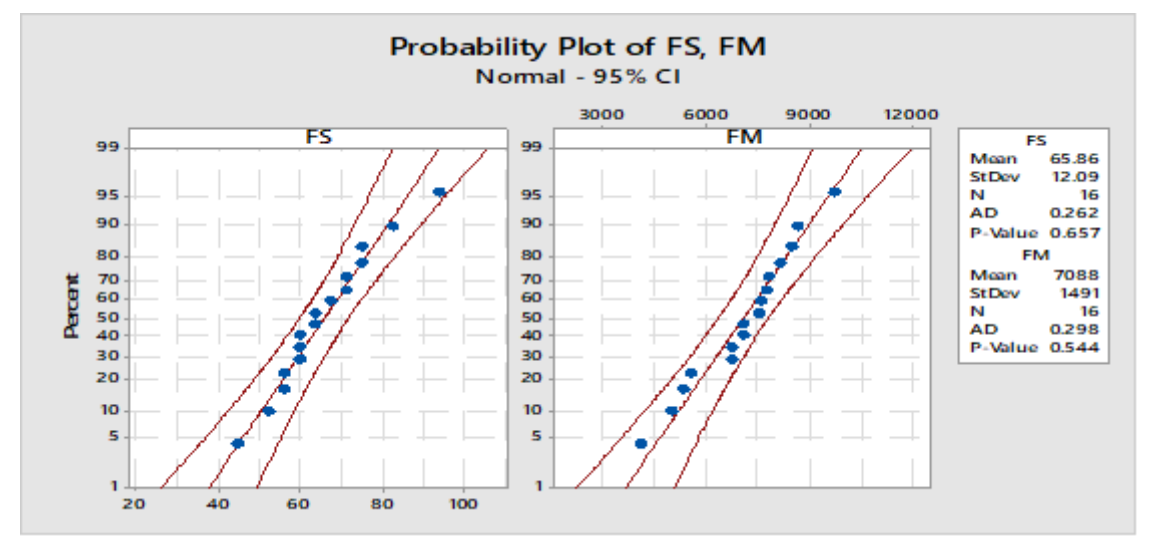


Fig. 1.: Probability plot for flexural strength (a) and flexural modulus (b) of samples

C. S/N Ratio Analysis of FS and FM

Tables IV and V present responses for the S/N ratio of flexural strength and flexural modulus, respectively. The delta value shows the significance of the control variables and helps to identify the optimal setting that generates higher flexural strength and modulus. The higher values of delta show the more significant variable, and based on values of delta, the whole significant variables are ranked properly. The value of delta ranking in Table IV indicates the MTT content as the most significant parameter in influencing the flexural strength of the biocomposite, followed by MCC content, and then S and T, respectively. The value of delta ranking in Table V indicates that the MTT is the highest significant factor in influencing the flexural modulus of the biocomposite, followed by MCC content, and then S and T, respectively.

Table IV: Response table for s/n ratios of fs (the larger the better)

Level	MCC	MTT	S	T
1	36.45	34.78	35.90	35.99
2	37.39	35.93	35.80	36.16
3	36.46	36.65	37.01	36.18
4	34.66	37.60	36.25	36.62
Delta	2.73	2.82	1.21	0.63
Rank	2	1	3	4
Delta	2.73	2.82	1.21	0.63

DOI: https://doi.org/10.59122/174CFC14



Table V: Response table for s/n ratios of FM (the larger the better)

Level	MCC	MTT	S	T
1	75.22	74.41	76.45	76.64
2	77.32	76.70	76.47	76.53
3	77.49	77.46	77.80	76.82
4	77.21	78.67	76.53	77.25
Delta	2.27	4.26	1.35	0.72
Rank	2	1	3	4

The S/N Ratio graphs are plotted for flexural strength and flexural modulus responses in Fig. 2. (a) and (b). The graph is drawn using the optimal control factors, and the optimal value is the one with the highest value of mean SNR. It has been found that the maximum flexural strength was obtained for developed biocomposite at 3%MCC, 9%MTT, 20%S, and 175°C T as shown in Fig. 2. (a). At this level, FS is 96.5 MPa. For flexural modulus, 6%MCC, 9%MTT, the 20S, and 175C showed the maximum S/N ratio as shown in Fig. 2. (b), and at this level FM is 9.8 GPa.

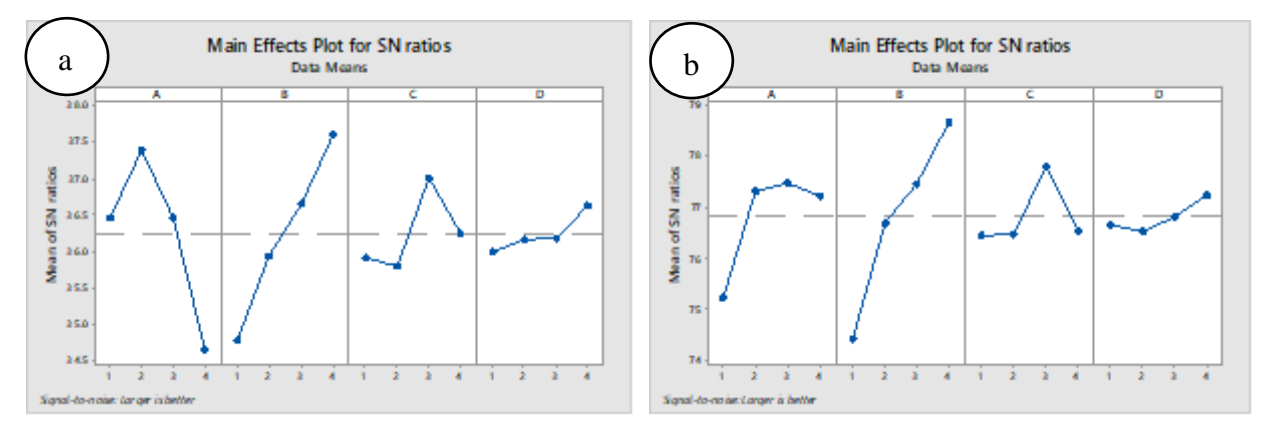


Fig. 2.: Main effect plot for S/N ratios of FS (a) and FM (b)

D. Regression Analysis

The relationship between factors that affect the flexural responses and outcomes is expressed by using the regression equation as follows:-

$$FS = 51.80 - 4.78 MCC + 7.03 MTT + 2.16 S + 1.22 T$$
 (8)

$$FM = 2.997 + 0.450 MCC + 1.039 MTT + 0.074 S + 0.074 T$$
 (9)

(P): 2959-393X DOI: https://doi.org/10.59122/174CFC14



Copyright and License Grant: CC By 4.0



Table VI presents the significance of factors incorporated in the regression equation of flexural strength. Table VI clearly shows that the regression P-value 0.005 suggests that the factors incorporated in the experimental setup are statistically highly significant for the linear model, and factors with a P-value less than 0.05 show the most significant parameter that influences the regression equation. Additionally, the larger F-value shows the more significant factor that influences the regression response. Table VI exhibits that MTT and MCC P-values are 0.002 and 0.016, respectively. This indicates that they are the most significant factors that affect the regression model of biocomposite flexural strength, and factors T and S have less significance, respectively.

Table VI: ANOVA for regression model of FS

Source	DF	Seq SS	Adj SS	Adj MS	F-Value	P-Value
Regression	4	1568.67	1568.67	392.17	6.91	0.005
MCC	1	457.21	457.21	457.21	8.06	0.016
MTT	1	988.77	988.77	988.77	17.42	0.002
S	1	92.99	92.99	92.99	1.64	0.227
T	1	29.71	29.71	29.71	0.52	0.484
Error	11	624.20	624.20	56.75		
Total	15	2192.87				

Table VII presents the significance of factors incorporated in the regression equation of flexural modulus. Table VII indicates that regression P-value 0.001 suggests that the factors incorporated in the model are statistically highly significant and factors MTT and MCC with P-value s of 0.000 and 0.033, respectively are the most significant factors that affect the regression model of biocomposite flexural modulus, and factor S and T have less significances, respectively.

Table VII: ANOVA for regression model of FM

Source	DF	Seq SS	Adj SS	Adj MS	F-Value	P-Value
Regression	4	25.855	25.855	6.463	9.47	0.001
MCC	1	4.042	4.042	4.042	5.92	0.033
MTT	1	21.594	21.594	21.594	31.63	0.000
S	1	0.110	0.110	0.110	0.16	0.695
T	1	0.108	0.108	0.108	0.16	0.698
Error	11	7.509	7.509	0.682		
Total	15	33.365				

Received: July 2024; Revised: 29 November 2024; Accepted: 15 December 2024; Published: 23 December 2024





E. Tensile Strength and Young Modulus of Biocomposite

Table VIII presents different specimen configurations of PLA-based biocomposites with various loadings of plasticizer, MCC and MTT contents, and temperature to analyze tensile strength and young modulus properties as responses and all data converted to S/N ratio also shown in Table VIII. From Table VIII, it is observed that the loading of S, MCC, and MTT improves the tensile strength of PLA. The experimental setup 6MCC/9MTT/10S/100T combination shows the highest tensile strength followed by 9MCC/6MTT/10S/175T, and experimental combination 6MCC/0MTT/20S/175T shows the lowest tensile strength following the neat PLA. The highest tensile strength experimental setup 6MCC/9MTT/10S/100T biocomposite has 83.3 MPa, which is 50 % greater than that of the neat PLA. It is easily assumed that in these contents, the fillers are dispersed uniformly within the PLA material [56]. The lowest biocomposite combination improves by 5% greater than that of the neat PLA. This is probably because the absence of MTT and increment of S reduces the tensile strength relative to the rest of the experimental setup [57]. As presented in Table VIII, the addition of fillers improves the modulus of elasticity of the neat PLA and plasticizer reduces the modulus of elasticity of neat PLA [58]. Therefore, the tradeoff is conducted to gain the optimal level of parameters. The minor inclusion of fillers without plasticizer at higher temperatures shows the highest young modulus at experiment 6 (3MCC/3MTT/0S/175T) with the value of 4.28 GPa. In this experimental combination, the Young's modulus is increased by 23% more than the neat PLA. This improvement is caused by the presence of MCC and MTT contents which restrict the molecular chain movement in the PLA and form physical and chemical interlocks with the PLA matrix.

Table VIII: Experimental setup and results of TS and YM with S/N ratio

	Factors				Responses				
S. N	MCC	MMT	S	T	TS (MPa)	S/N Ratio	YS (GPa)	S/N Ratio	
1	0	0	0	100	55.5	34.8945	3.28	10.3175	
2	0	3	10	125	68.8	36.7630	3.60	11.1261	
3	0	6	20	150	72.2	37.1734	3.93	11.8879	
4	0	9	30	175	77.7	37.8171	3.70	11.364	
5	3	0	10	150	66.6	36.4782	3.38	10.5783	
6	3	3	0	175	77.7	37.8171	4.26	12.5882	
7	3	6	30	100	67.7	36.6217	3.44	10.7312	
8	3	9	20	125	75.5	37.5653	3.53	10.9555	
9	6	0	20	175	58.3	35.3178	3.12	9.8831	
10	6	3	30	150	72.2	37.1734	3.75	11.4806	

0

DOI: https://doi.org/10.59122/174CFC14



11	6	6	0	125	78.8	37.9403	4.13	12.319	
12	6	9	10	100	83.3	38.4164	3.95	11.9319	
13	9	0	30	125	66.6	36.4773	2.55	8.1308	
14	9	3	20	100	70.5	36.9706	2.63	8.3991	
15	9	6	10	175	81.6	38.2409	2.89	9.218	
16	9	9	0	150	78.8	37.9403	3.21	10.1301	

The best S/N ratio shown in Table VIII for TS is 38.41 at experiment number 12 and also offers the highest TS value of 83.3 MPa. The weakest S/N ratio is 34.89 observed in experiment 1. The best S/N ratio of YM is observed in experiment 6 with a value of 12.58 and the weakest S/N ratio is observed in experiment 13 with a value of 8.13.

F. Probability Plot

The probability plot shows each value of the experimental setup against the percentage of values in the specimen that are less than or equal to it, along a fitted distribution line. Fig. 3 exhibits that all sample values are under normal distribution at the confidence level of 95%. The two lines beside the center line on the left and right show the upper and lower limits of the confidence interval. No sample value is out of the confidence interval. This tendency offers improved outcomes for future estimation of process characteristics.

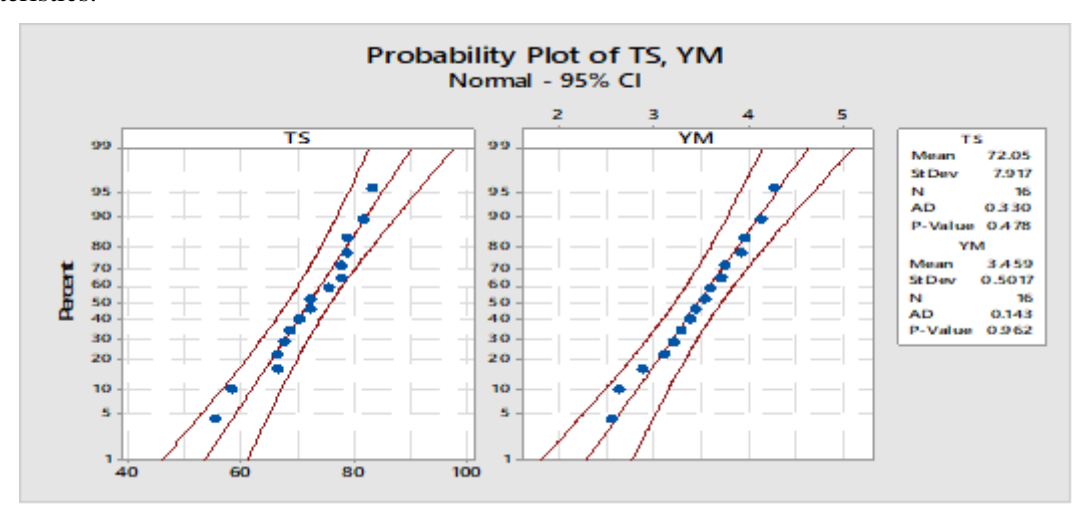


Fig. 3.: Probability plot of FS and YM

G. Signal to Noise Ratio Analysis of Tensile strength and Young modulus

Table VIII shows the S/N ratios of TS for the greater the better characteristic to maximize the tensile strength of biocomposite material. The optimal experimental setup for the larger the better tensile strength characteristics is 9%MCC, 9%MTT, 10%S, and 175°C. At this level, the TS is 85.2 MPa and MTT primarily



Copyright and License Grant: CC By 4.0



affects the tensile strength followed by MCC, S, and T, respectively. The main effects plot for S/N ratios of TS is presented in Fig. 4 (a).

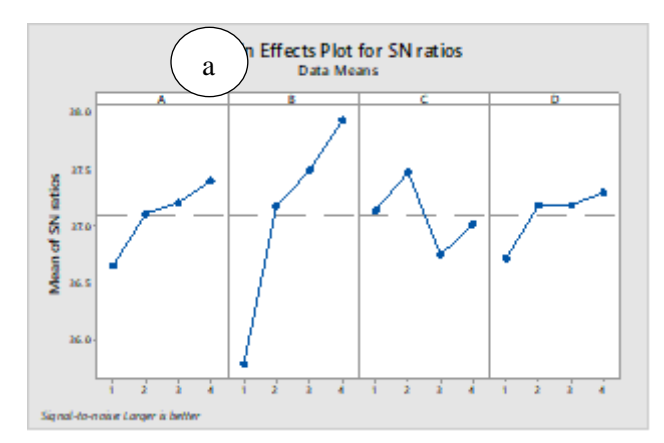
Table IX: Response table for S/noise ratios of TS (the larger the better)

Level	MCC	MTT	S	T
1	36.66	35.79	37.15	36.73
2	37.12	37.18	37.47	37.19
3	37.21	37.49	36.76	37.19
4	37.41	37.93	37.02	37.30
Delta	0.75	2.14	0.72	0.57
Rank	2	1	3	4

Table X presents the S/N ratios of the Young modulus of biocomposites. The optimal experimental setup for the larger the better characteristics of young modulus is 6%MCC, 9%MTT, 0%S, and 150°C. At this level, the YM is 4.28 GPa and is primarily affected by MCC followed by MTT, S, and T, respectively. The main effects plot for S/N ratios of Young modulus is presented in Fig. 4 (b).

Table X: Response table for S/N ratios of Young's modulus (the larger the better)

Level	MCC	MTT	S	T
1	11.174	9.727	11.339	10.345
2	11.213	10.898	10.714	10.633
3	11.404	11.039	10.281	11.019
4	8.969	11.095	10.427	10.763
Delta	2.434	1.368	1.057	0.674
Rank	1	2	3	4



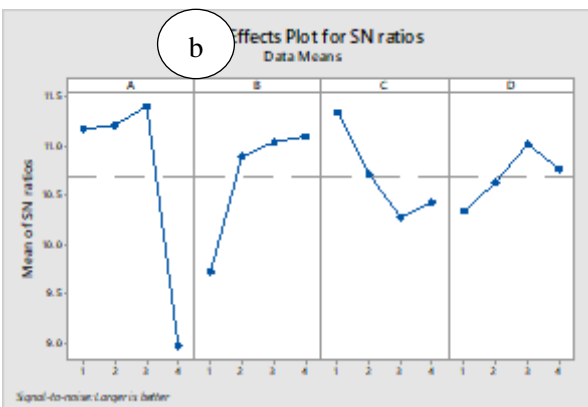


Fig. 4: Main effects plot for S/N ratios of tensile strength (a) and young modulus (b)

Received: July 2024; Revised: 29 November 2024; Accepted: 15 December 2024; Published: 23 December 2024





H. Regression Analysis

The regression analysis is a statistical technique that explains the correlation between factors and one or more responses. The relations tensile strength and young modulus have with the input parameters, i.e. MCC content, MTT content, S content, and temperature are given by regression equation as follows;

$$TS = 53.16 + 1.87 MCC + 5.40 MTT - 1.10 S + 1.37 T$$
 (10)
 $YM = 3.802 - 0.2338 MCC + 0.1583 MTT - 0.1232 S + 0.0618 T$ (11)

ANOVA for regression model of TS and YM of biocomposite

The significance of factors incorporated in the regression equation of tensile strength is given in ANOVA Table XI. The regression P-value (0.002) lesser than 0.05 suggests that a statistically significant relationship occurs between factors and responses in the experimental design. And factors' P-value lesser than 0.05 shows the most significant parameter that influences the regression equation. Additionally, the larger F-value shows the more significant factor that influences the response. Table XI presents that MTT P-value 0.000 and F-value 28.68 indicate that MTT is the most significant factor for the regression model of tensile strength, and factors MCC, T, and S have less and less significance, respectively.

Table XI: ANOVA for regression equation of TS

Source	DF	Adj SS	Adj MS	F-Value	P-Value
Regression	4	716.14	179.04	8.79	0.002
MCC	1	70.27	70.27	3.45	0.090
MTT	1	583.96	583.96	28.68	0.000
S	1	24.10	24.10	1.18	0.300
T	1	37.81	37.81	1.86	0.200
Error	11	223.97	20.36		
Total	15	940.11			

Table XII presents the significance of factors incorporated in the regression equation of the Young's modulus. Table XII clearly shows that regression P-value 0.066 suggests that the factors incorporated in the experimental setup are satisfactory for the linear model because factors with a P-value lesser than 0.05 show the most significant parameter that influences the regression equation. Additionally, the larger F-value shows the more significant factor that influences the regression response. Table XII exhibits that MCC P-value 0.025 and F-value 6.67 indicate that MCC is the most significant factor that affects the regression model of biocomposite young modulus, and factors MTT, S, and T have less and less significance, respectively.



Copyright and License Grant: CC By 4.0



Table XII: ANOVA for regression model of YM

Source	DF	Seq SS	Adj SS	Adj MS	F-Value	P-Value
Regression	4	1.97372	1.97372	0.49343	3.01	0.066
MCC	1	1.09278	1.09278	1.09278	6.67	0.025
MTT	1	0.50086	0.50086	0.50086	3.06	0.108
S	1	0.30381	0.30381	0.30381	1.85	0.200
T	1	0.07626	0.07626	0.07626	0.47	0.509
Error	11	1.80158	1.80158	0.16378		
Total	15	3.77529				

I. Water Absorption and Density

Table XIII displays the water absorption and density of the developed biocomposite. Underwater absorption, as observed in Table XIII, the combination of MCC, MTT, and S addition highly influences the water absorption of PLA. The experimental setup of higher levels of MCC and S such as 6MCC/3MTT/30S/150T and 9MCC/0MTT/30S/125T, indicated higher water absorptions of 15.17 and 16.22 %, respectively. This is caused mainly because MCC and S have high water absorption trends [59]. Additionally, the water absorption rises with temperature due to the molecular processes. An increase in non-equilibrium vapor pressure at the interface leads to greater absorption of water molecules by the fiber. This phenomenon, associated with a reduction in solid—gas interfacial tension, enhances water absorption [60]. Under the density, the addition of MCC, MTT, and S slightly increases the density of PLA. In related studies, the addition of natural fiber (MTT and MCC) in PLA increases the density of PLA, this is probably due to the high densities of fillers [61].

Table XIII: Water absorption and density of biocomposite with S/N ratios

		Fact	ors		Responses				
S. N	MCC	MMT	S	T	Water absorption (%)	S/N Ratio	Density (g/mm ³)	S/N Ratio	
1	0	0	0	100	2.48	-7.91	0.0303	-30.371	
2	0	3	10	125	6.03	-15.60	0.0331	-29.617	
3	0	6	20	150	8.78	-18.87	0.0348	-29.164	

Received: July 2024; Revised: 29 November 2024; Accepted: 15 December 2024; Published: 23 December 2024



Copyright and License Grant: CC By 4

)	(00)	•	
	\smile	BY	

4	0	9	30	175	10.63	-20.53	0.0384	-28.311
5	3	0	10	150	5.54	-14.87	0.0331	-29.608
6	3	3	0	175	4.19	-12.46	0.0342	-29.327
7	3	6	30	100	12.32	-21.81	0.0332	-29.569
8	3	9	20	125	7.81	-17.86	0.0362	-28.838
9	6	0	20	175	9.73	-19.76	0.0364	-28.771
10	6	3	30	150	15.22	-23.65	0.0376	-28.508
11	6	6	0	125	5.11	-14.17	0.0353	-29.038
12	6	9	10	100	6.94	-16.83	0.0381	-28.378
13	9	0	30	125	16.17	-24.17	0.0362	-28.826
14	9	3	20	100	10.02	-20.02	0.0371	-28.609
15	9	6	10	175	7.28	-17.24	0.0393	-28.123
16	9	9	0	150	6.86	-16.73	0.0415	-27.639

J. Probability Plot

The normal probability plot shown in Fig. 5 represents the comparison between the actual experimental results and the predicted values of water absorption and density. As clearly shown in Fig. 5 all the experimental data are under the interval of 95% confidence level.

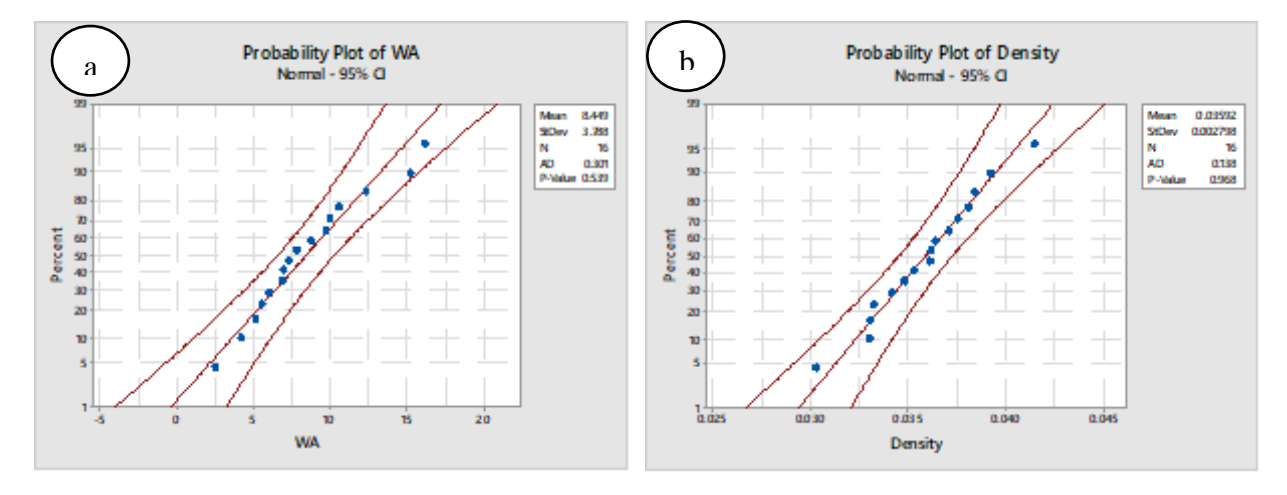


Fig. 5.: Probability plot for water absorption (a) and density (b) of developed biocomposite

As Table XIV and Table XV show, based on the S/N ratio result, it can be examined which factor has the highest influence on water absorption and density, respectively. The optimal water absorption factor of these controlled variables is investigated based on S/N ratios shown in Table XIV and Fig. 6 (a). The optimal factor for WA is at the combination of 0%MCC, 0%MTT, 0%S, and 150°C, and at this level, the WA is 2.42 %. The factors that highly affect water absorption are S and MCC, respectively. This is mainly due to a lot of hydroxyl (-OH) groups in these constituents [62]. The optimization of water absorption



Copyright and License Grant: CC By 4.0



factors, based on the criterion that 'smaller is better,' indicates that lower levels of fillers and plasticizers are most effective, as shown in Fig. 6(a). Table XV and Fig. 6(b) reveal the optimal factors for density, identified at 9MCC/9MTT/30S/175T. At this level, the density is determined to be 0.0427 g/mm³.

Table XIV: Response table for S/N ratios of water absorption (the smaller the better)

Level	MCC	MTT	S	T
1	-15.73	-16.68	-12.82	-16.65
2	-16.75	-17.94	-16.14	-17.96
3	-18.61	-18.03	-19.13	-18.53
4	-19.55	-17.99	-22.54	-17.50
Delta	3.81	1.35	9.72	1.89
Rank	2	4	1	3

Table XV: Response table for S/N ratios of density (the larger the better)

Level	MCC	MTT	S	T
1	-29.37	-29.39	-29.09	-29.23
2	-29.34	-29.02	-28.93	-29.08
3	-28.67	-28.97	-28.85	-28.73
4	-28.30	-28.29	-28.80	-28.63
Delta	1.07	1.10	0.29	0.60
Rank	2	1	4	3

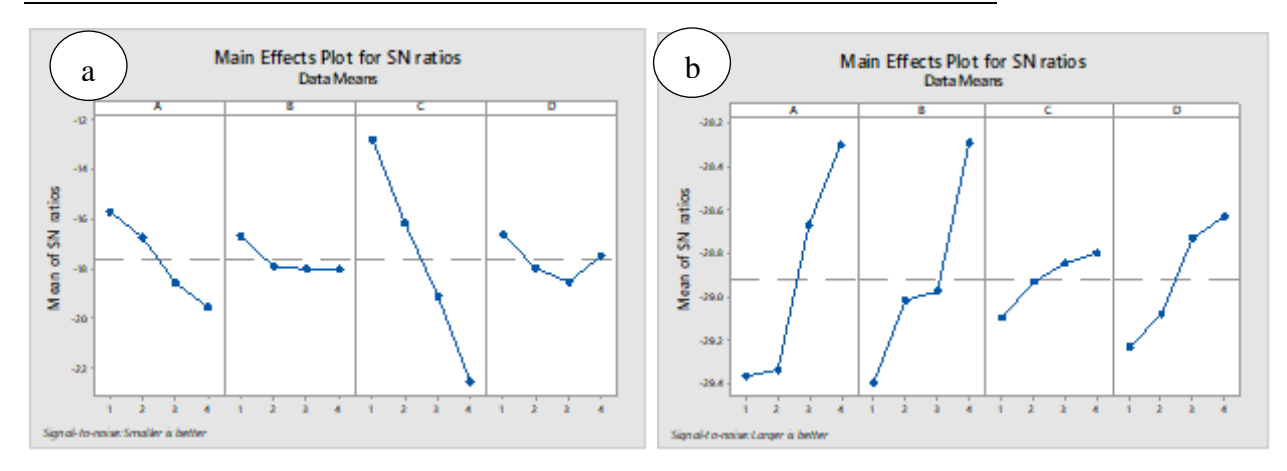


Fig. 6.: Main effect plot for S/N ratios of water absorption (a) and density (b)



Copyright and License Grant: CC By 4.0



K. Regression Analysis of Correlation between Significant Factors and Water Absorption

The correlation between significant factors and the water absorption of developed biocomposite is established through linear regression. The regression equation for the water absorption is shown as follows;

$$WA = -1.33 + 1.110 MCC - 0.175 MTT + 2.941 S + 0.037 T$$
 (12)

Density =
$$0.02551 + 0.001581 \text{ MCC} + 0.001381 \text{ MTT} + 0.000332 \text{ S} + 0.000868 \text{ T}$$
 (13)

ANOVA for regression model of water absorption and density of developed biocomposite

The significance of factors incorporated in the regression equation of water absorption and density is given in ANOVA Tables XVI and XVII, respectively. The regression P-value (0.000) suggests that a statistically significant relationship occurs between factors and responses in the experimental design, and factors with a P-value lesser than 0.05 show the most significant element that influences the regression equation. Table 16 presents that S and MCC are the most significant factors for the regression model of water absorption. Table XVII presents that MCC, MTT, and T are the most significant factors for the regression model of density.

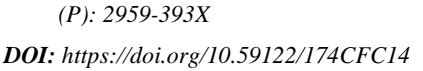
Table XVI: ANOVA for regression model of water absorption

Source	DF	Seq SS	Adj SS	Adj MS	F-Value	P-Value
Regression	4	198.222	198.222	49.555	32.11	0.000
MCC	1	24.635	24.635	24.635	15.96	0.002
MTT	1	0.611	0.611	0.611	0.40	0.542
S	1	172.948	172.948	172.948	112.06	0.000
T	1	0.027	0.027	0.027	0.02	0.897
Error	11	16.977	16.977	1.543		
Total	15	215.199				

Table XVII: Analysis of variance for regression model of density

DF	Seq SS	Adj SS	Adj MS	F-Value	P-Value
4	0.000105	0.000105	0.000026	24.09	0.000
1	0.000050	0.000050	0.000050	45.73	0.000
1	0.000038	0.000038	0.000038	34.86	0.000
1	0.000002	0.000002	0.000002	2.02	0.183
1	0.000015	0.000015	0.000015	13.76	0.003
11	0.000012	0.000012	0.000001		
15	0.000117				
	4 1 1 1 1 1	4 0.000105 1 0.000050 1 0.000038 1 0.000002 1 0.000015 11 0.000012	4 0.000105 0.000105 1 0.000050 0.000050 1 0.000038 0.000038 1 0.000002 0.000002 1 0.000015 0.000015 11 0.000012 0.000012	4 0.000105 0.000105 0.000026 1 0.000050 0.000050 0.000050 1 0.000038 0.000038 0.000038 1 0.000002 0.000002 0.000002 1 0.000015 0.000015 0.000001 11 0.000012 0.000012 0.000001	4 0.000105 0.000105 0.000026 24.09 1 0.000050 0.000050 0.000050 45.73 1 0.000038 0.000038 0.000038 34.86 1 0.000002 0.000002 0.000002 2.02 1 0.000015 0.000015 0.000015 13.76 11 0.000012 0.000012 0.000001





ISSN (E): 2959-3921



IV. Conclusion

This study investigated the optimization of PLA-based biocomposite material development using the application of Taguchi and regression model analysis. The fillers namely MCC and MTT, and Plasticizer S at various weight % loadings were considered with different T. Based on the experimental studies' results, the following conclusions could be made:-

- 1. The optimal factors in flexural strength are at 3%MCC, 9%MTT, 20%S, and 175°C. At these levels, FS is 96.5 MPa whereas for flexural modulus, 6%MCC, 9%MTT, 20%S, and 175°C. At these control factors, FM is 9.8 GPa.
- 2. The optimal factors in tensile strength are at 9%MCC, 9%MTT, 10%S, and 175°C. At these levels, TS is 85.2 MPa whereas for tensile modulus, 6%MCC, 9%MTT, 0%S, and 150°C. At these experimental runs, YM is 4.22 GPa
- 3. The optimal factors in hardness value are at 6%MCC, 9%MTT, 10%S, and 175°C. At these levels, HV is 138.2.
- 4. The optimal factors in water absorption are at 0%MCC, 0%MTT, 0%S, and 150°C. At these experimental runs, WA is 2.42% whereas for density, 9%MCC, 9%MTT, 30%S, and 175°C. At this experimental setup, D is 0.0427g/mm³.

Finally, it was concluded that the inclusion of MCC, MTT, and S highly influences the performance characteristics of PLA. The PLA-based biocomposite developed using this approach is expected to be utilized for lightweight load-carrying applications

References

- O. S. Onyekwere, M. H. Oladeinde, and R. O. Edokpia, "Multi-Response optimization of bamboo fiber reinforced unsaturated polyester composites using hybrid Taguchi-grey relational analysis method," *Journal of Industrial and Production Engineering*, vol. 38, no. 2, pp. 98-107, 2021. DOI: 10.1080/21681015.2020.1848933.
- 2. T. Manu, A. R. Nazmi, B. Shahri, N. Emerson, and T. Huber, "Biocomposites: A Review of Materials and Perception," *Materials Today Communications*, vol. 31, art. no. 103308, 2022. DOI: 10.1016/j.mtcomm.2022.103308.
- 3. M. Belkheir, M. Boutaleb, A. Mokaddem, and B. Doumi, "Predicting the effect of coconut natural fibers for improving the performance of biocomposite materials based on the poly (methyl methacrylate)-PMMA polymer for engineering applications," *Polymer Bulletin*, Issue 2, 2023. DOI: 10.1007/s00289-020-03183-7.



- 4. A. A. Mohammed, A. A. B. Omran, Z. Hasan, R. Ilyas, and S. Sapuan, "Wheat biocomposite extraction, structure, properties and characterization: a review," *Polymers*, vol. 13, no. 21, p. 3624, 2021. DOI: 10.3390/polym13213624.
- 5. V. Naik and M. Kumar, "A review on natural fiber composite material in automotive applications," *Engineered Science*, vol. 18, pp. 1-10, 2021. DOI: 10.30919/es8d589.
- 6. S. Bhambure and A. Rao, "Experimental investigation of impact strength of kenaf fiber reinforced polyester composite," *Materials Today: Proceedings*, vol. 46, Part 2, pp. 1134-1138, 2021. DOI: 10.1016/j.matpr.2021.02.055.
- M. R. Ketabchi, M. Khalid, C. T. Ratnam, S. Manickam, R. Walvekar, and M. E. Hoque, "Sonosynthesis of cellulose nanoparticles (CNP) from kenaf fiber: effects of processing parameters," *Fibers and Polymers*, vol. 17, no. 9, pp. 1352-1358, 2016. DOI: 10.1007/s12221-016-5813-4.
- 8. A. El Amri, A. Ouass, Z. Wardighi, F. Z. Bouhassane, A. Zarrouk, A. Habsaoui, et al., "Extraction and characterization of cellulosic nanocrystals from stems of the reed plant large-leaved cattail (Typha latifolia)," *Materials Today: Proceedings*, 2022. DOI: 10.1016/j.matpr.2022.08.408
- 9. S. H. Sung, Y. Chang, and J. Han, "Development of polylactic acid nanocomposite films reinforced with cellulose nanocrystals derived from coffee silverskin," *Carbohydrate Polymers*, vol. 169, pp. 495-503, 2017. DOI: 10.1016/j.carbpol.2017.04.037.
- A. Khenblouche, D. Bechki, M. Gouamid, K. Charradi, L. Segni, M. Hadjadj, and S. Boughali, "Extraction and characterization of cellulose microfibers from Retama raetam stems," *Polímeros*, vol. 29, no. 1, 2019. DOI: 10.1590/0104-1428.05218.
- J. I. Morán, V. A. Alvarez, V. P. Cyras, and A. Vázquez, "Extraction of cellulose and preparation of nanocellulose from sisal fibers," *Cellulose*, vol. 15, no. 1, pp. 149-159, 2008. DOI: 10.1007/s10570-007-9145-9.
- A. Kausar, S. T. Zohra, S. Ijaz, M. Iqbal, J. Iqbal, I. Bibi, S. Nouren, N. El Messaoudi, and A. Nazir, "Cellulose-based materials and their adsorptive removal efficiency for dyes: A review," *International Journal of Biological Macromolecules*, vol. 224, pp. 1337-1355, 2023. DOI: 10.1016/j.ijbiomac.2022.10.220.
- 13. M. Szymańska-Chargot, J. Cieśla, P. Pękala, P. M. Pieczywek, W. Oleszek, M. Żyła, Z. Szkopek, and A. Zdunek, "The Influence of High-Intensity Ultrasonication on Properties of Cellulose Produced from the Hop Stems, the Byproduct of the Hop Cones Production," *Molecules*, vol. 27, no. 9, p. 2624, 2022. DOI: 10.3390/molecules27092624.



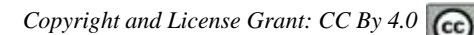
- N. Reddy and Y. Yang, "Extraction and characterization of natural cellulose fibers from common milkweed stems," *Polymer Engineering & Science*, vol. 49, no. 11, pp. 2212-2217, 2009. DOI: 10.1002/pen.21469.
- N. M. Zeleke, D. K. Sinha, and G. A. Mengesha, "Chemical Composition and Extraction of Micro Crystalline Cellulose from Outer Skin Isolated Coffee Husk," *Advances in Materials Science and Engineering*, vol. 2022, Article ID 7163359, 2022. DOI: 10.1155/2022/7163359.
- H. S. Hafid, F. N. Omar, J. Zhu, and M. Wakisaka, "Enhanced crystallinity and thermal properties of cellulose from rice husk using acid hydrolysis treatment," *Carbohydrate Polymers*, vol. 260, Article ID 117789, 2021. DOI: 10.1016/j.carbpol.2021.117789.
- 17. G. Manimekalai, S. Kavitha, D. Divya, S. Indran, and J. Binoj, "Characterization of enzyme treated cellulosic stem fiber from Cissus quadrangularis plant: an exploratory investigation," *Current Research in Green and Sustainable Chemistry*, vol. 4, Article ID 100162, 2021. DOI: 10.1016/j.crgsc.2021.100162.
- D. Trache, M. H. Hussin, C. T. H. Chuin, S. Sabar, M. N. Fazita, O. F. Taiwo, et al., "Microcrystalline cellulose: Isolation, characterization and bio-composites application—A review," *International Journal of Biological Macromolecules*, vol. 93(Pt A), pp. 789-804, 2016. DOI: 10.1016/j.ijbiomac.2016.09.056.
- D. Haldar and M. K. Purkait, "Micro and nanocrystalline cellulose derivatives of lignocellulosic biomass: A review on synthesis, applications, and advancements," *Carbohydrate Polymers*, vol. 250, Article ID 116937, 2020. DOI: <u>10.1016/j.carbpol.2020.116937</u>.
- 20. H. S. Shekar and M. Ramachandra, "Green composites: a review," *Materials Today: Proceedings*, vol. 5, no. 1, Part 3, pp. 2518-2526, 2018. DOI: 10.1016/j.matpr.2017.11.387.
- 21. M. Zwawi, "A Review on Natural Fiber Bio-Composites, Surface Modifications and Applications," *Molecules*, vol. 26, no. 2, p. 404, 2021. DOI: <u>10.3390/molecules26020404</u>.
- 22. B. Debnath, D. Haldar, and M. K. Purkait, "A critical review on the techniques used for the synthesis and applications of crystalline cellulose derived from agricultural wastes and forest residues," *Carbohydrate Polymers*, vol. 273, Article ID 118537, 2021. DOI: 10.1016/j.carbpol.2021.118537.
- 23. G. Wang, D. Zhang, B. Li, G. Wan, G. Zhao, and A. Zhang, "Strong and thermal-resistance glass fiber-reinforced polylactic acid (PLA) composites enabled by heat treatment," *International Journal of Biological Macromolecules*, vol. 129, pp. 448-459, 2019. DOI: 10.1016/j.ijbiomac.2019.01.123.



- 24. K. Pongtanayut, C. Thongpin, and O. Santawitee, "The effect of rubber on morphology, thermal properties and mechanical properties of PLA/NR and PLA/ENR blends," *Energy Procedia*, vol. 34, pp. 888-897, 2013. DOI: 10.1016/j.egypro.2013.06.826.
- 25. A. Greco and F. Ferrari, "Thermal behavior of PLA plasticized by commercial and cardanol-derived plasticizers and the effect on the mechanical properties," *Journal of Thermal Analysis and Calorimetry*, vol. 146, no. 1, pp. 131-141, 2021. DOI: 10.1007/s10973-020-10403-9.
- M. Puthumana, P. Santhana Gopala Krishnan, and S. K. Nayak, "Chemical modifications of PLA through copolymerization," *International Journal of Polymer Analysis and Characterization*, vol. 25, no. 8, pp. 634-648, 2020. DOI: 10.1080/1023666X.2020.1830650.
- 27. K. Martinez Villadiego, M. J. Arias Tapia, J. Useche, and D. Escobar Macías, "Thermoplastic starch (TPS)/polylactic acid (PLA) blending methodologies: a review," *Journal of Polymers and the Environment*, vol. 30, no. 1, pp. 75-91, 2022. DOI: 10.1007/s10924-021-02207-1.
- 28. G. Rajeshkumar, S. A. Seshadri, G. Devnani, M. Sanjay, S. Siengchin, J. P. Maran, et al., "Environment-friendly, renewable and sustainable poly lactic acid (PLA) based natural fiber reinforced composites—A comprehensive review," *Journal of Cleaner Production*, vol. 310, Article ID 127483, 2021. DOI: 10.1016/j.jclepro.2021.127483.
- 29. R. Guo, Z. Ren, H. Bi, M. Xu, and L. Cai, "Electrical and thermal conductivity of polylactic acid (PLA)-based biocomposites by incorporation of nano-graphite fabricated with fused deposition modeling," *Polymers*, vol. 11, no. 3, p. 549, 2019. DOI: 10.3390/polym11030549.
- 30. M. Bocqué, C. Voirin, V. Lapinte, S. Caillol, and J.-J. Robin, "Petro-based and bio-based plasticizers: chemical structures to plasticizing properties," *Journal of Polymer Science Part A: Polymer Chemistry*, vol. 54, no. 1, pp. 11-33, 2016. DOI: 10.1002/pola.27917.
- 31. A. Alhanish and M. Abu Ghalia, "Developments of biobased plasticizers for compostable polymers in the green packaging applications: A review," *Biotechnology Progress*, vol. 37, no. 6, p. e3210, 2021. DOI: 10.1002/btpr.3210.
- 32. M. G. A. Vieira, M. A. da Silva, L. O. dos Santos, and M. M. Beppu, "Natural-based plasticizers and biopolymer films: A review," *European Polymer Journal*, vol. 47, no. 3, pp. 254-263, 2011. DOI: 10.1016/j.eurpolymj.2010.12.011.
- 33. M. Shahmaleki, F. Beigmohammadi, and F. Movahedi, "Cellulose-Reinforced Starch Biocomposite: Optimization of the Effects of Filler and Various Plasticizers using Design–Expert Method," *Stärke*, vol. 73, no. 9-10, Article ID 2000028, 2021. DOI: 10.1002/star.202000028.



- 34. M. Liu, Y. Zhou, Y. Zhang, C. Yu, and S. Cao, "Physicochemical, mechanical and thermal properties of chitosan films with and without sorbitol," *International Journal of Biological Macromolecules*, vol. 70, pp. 340-346, 2014. DOI: <u>10.1016/j.ijbiomac.2014.06.050</u>.
- 35. X. Ma, C. Qiao, J. Zhang, and J. Xu, "Effect of sorbitol content on microstructure and thermal properties of chitosan films," *International Journal of Biological Macromolecules*, vol. 119, pp. 1294-1297, 2018. DOI: 10.1016/j.ijbiomac.2018.08.034.
- 36. R. Rafiee and R. Shahzadi, "Mechanical properties of nanoclay and nanoclay reinforced polymers: a review," *Polymer Composites*, vol. 40, no. 2, pp. 431-445, 2019. DOI: 10.1002/pc.24747.
- 37. M. S. Nazir, M. H. Mohamad Kassim, L. Mohapatra, M. A. Gilani, M. R. Raza, and K. Majeed, "Characteristic properties of nano clays and characterization of nanoparticles and nanocomposites," in *Nanoclay Reinforced Polymer Composites: Nanocomposites and bionanocomposites*, M. Jawaid, A. el K. Qaiss and R. Bouhfid, Eds. Singapore: Springer Science Business Media Singapore, 2016, pp. 35-55. DOI: 10.1016/B978-0-323-39390-0.00002-4.
- 38. A. U. R. Shah, M. Prabhakar, and J.-I. Song, "Current advances in the fire retardancy of natural fiber and bio-based composites—A review," *International Journal of Precision Engineering and Manufacturing-Green Technology*, vol. 4, no. 2, pp. 247-262, 2017. DOI: 10.1007/s40684-017-0029-1.
- 39. G. Rajeshkumar, S. A. Seshadri, S. Ramakrishnan, M. Sanjay, S. Siengchin, and K. Nagaraja, "A comprehensive review on natural fiber/nano-clay reinforced hybrid polymeric composites: Materials and technologies," *Polymer Composites*, vol. 42, no. 8, pp. 3687-3701, 2021. DOI: 10.1002/pc.26125.
- 40. D. Rajamani, E. Balasubramanian, G. Dilli Babu, and K. Ananthakumar, "Experimental investigations on high precision abrasive waterjet cutting of natural fiber reinforced nano clay filled green composites," *Journal of Industrial Textiles*, vol. 51, no. 3, pp. 3786-3810, 2022. DOI: 10.1177/15280837211057684.
- 41. S. N. Shuvo, K. M. Shorowordi, and M. A. Islam, "Effect of nanoclay on jute fiber reinforced polyester composites," *International Journal of Advanced Engineering and Nano Technology*, vol. 2, no. 8, pp. 20-26, 2015. DOI: 10.2139/ssrn.2668083
- 42. J. Ferreira, L. Borrego, J. Costa, and C. Capela, "Fatigue behavior of nanoclay reinforced epoxy resin composites," *Composites Part B: Engineering*, vol. 52, pp. 286-291, 2013. DOI: 10.1016/j.compositesb.2013.04.003.





- 43. T. K. A. Bui, S. V. Hoa, T. D. Ngo, and M. T. T. That, "Effect of addition of nanoclays on properties of vinyl ester," in *Design, Manufacturing, and Applications of Composites: Proceedings of the Eighth Joint Canada-Japan Workshop on Composites*, 2010. DOI: 10.1007/978-1-4419-0733-5_10.
- 44. A. S. Alex, R. Rajeev, K. Krishnaraj, N. Sreenivas, S. Manu, C. Gouri, et al., "Thermal protection characteristics of polydimethylsiloxane-organoclay nanocomposite," *Polymer Degradation and Stability*, vol. 144, pp. 281-291, 2017. DOI: 10.1016/j.polymdegradstab.2017.08.026.
- 45. R. Kurda, J. de Brito, and J. D. Silvestre, "CONCRETop-A multi-criteria decision method for concrete optimization," *Environmental Impact Assessment Review*, vol. 74, pp. 73-85, 2019. DOI: 10.1016/j.eiar.2018.10.006.
- 46. H. Kus, G. Basar, and F. Kahraman, "Modeling and optimization for fly ash reinforced bronze-based composite materials using multi-objective Taguchi technique and regression analysis," *Industrial Lubrication and Tribology*, vol. 70, no. 7, pp. 1187-1192, 2018. DOI: 10.1108/ILT-02-2018-0059.
- 47. D. Jena, R. C. Mohapatra, and A. K. Das, "Optimization of mechanical characteristics of rice husk particle reinforced polymer composites using Taguchi Experimental Technique," *World Scientific News*, vol. 124, no. 2, pp. 155-170, 2019. DOI: 10.1108/ILT-02-2018-0059.
- 48. O. Kelleci, D. Aydemir, E. Altuntas, A. Oztel, R. Kurt, H. Yorur, et al., "Thermoplastic composites of polypropylene/biopolymer blends and wood flour: Parameter optimization with fuzzy-grey relational analysis," *Polymers and Polymer Composites*, vol. 30, 2022. DOI: 10.1177/09673911221100968.
- 49. C. C. Ihueze, M. K. Achike, and C. Okafor, "Optimal Performance Characteristics and Reinforcement Combinations of Coconut Fibre Reinforced High-Density Polyethylene (HDPE) Polymer Matrixes," *SSRN*, 2015. DOI: 10.2139/ssrn.2902118.
- 50. S. Budin, N. Maiden, M. Koay, D. Ibrahim, and H. Yusoff, "A comparison study on mechanical properties of virgin and recycled polylactic acid (PLA)," in *Journal of Physics: Conference Series*, 2019. DOI: 10.1088/1742-6596/1372/1/012002.
- 51. D. Chandramohan and A. J. P. Kumar, "Experimental data on the properties of natural fiber particle reinforced polymer composite material," *Data in Brief*, vol. 13, pp. 460-468, 2017. DOI: 10.1016/j.dib.2017.06.045
- 52. R. Ramasubbu and S. Madasamy, "Fabrication of automobile component using hybrid natural fiber reinforced polymer composite," *Journal of Natural Fibers*, vol. 19, no. 2, pp. 736-746, 2022. DOI: 10.1080/15440478.2020.1761927.



- 53. M. Kandasamy, A. Chandravathanan, and M. Mohan, "An investigation on tribological and mechanical properties of areca nut and BBorassus flabellifer fiber hybrid composite reinforced with epoxy," *Ind Eng J*, vol. 13, no. 2, 2020. DOI: <u>10.26488/iej.13.2.1217</u>.
- 54. S. Kormin, F. Kormin, and M. Beg, "Effect of plasticizer on physical and mechanical properties of LDPE/sago starch blend," in *Journal of Physics: Conference Series*, 2019. DOI: <u>10.1088/1742-6596/1150/1/012032</u>.
- 55. B. Dogu and C. Kaynak, "Behavior of polylactide/microcrystalline cellulose biocomposites: effects of filler content and interfacial compatibilization," *Cellulose*, vol. 23, pp. 611-622, 2016. DOI: 10.1007/s10570-015-0839-0.
- 56. R. Arjmandi, A. Hassan, M. K. Mohamad Haafiz, and Z. Zakaria, "Effects of micro- and nanocellulose on tensile and morphological properties of montmorillonite nano clay reinforced polylactic acid nanocomposites," in *Nanoclay Reinforced Polymer Composites: Natural Fibre/Nanoclay Hybrid Composites, M.* Jawaid, A. Qaiss, and R. Bouhfid, Eds. 2016, pp. 103-125. DOI: 10.1007/978-981-10-0950-1_5.
- 57. M. Arief, A. Mubarak, and D. Pujiastuti, "The concentration of sorbitol on bioplastic cellulose based carrageenan waste on biodegradability and mechanical properties bioplastic," in *IOP Conference Series: Earth and Environmental Science*, vol. 679, no. 1, Article ID 012013, 2021. DOI: 10.1088/1755-1315/679/1/012013.
- 58. H. Tian, D. Liu, Y. Yao, S. Ma, X. Zhang, and A. Xiang, "Effect of sorbitol plasticizer on the structure and properties of melt processed polyvinyl alcohol films," *Journal of Food Science*, vol. 82, no. 12, pp. 2926-2932, 2017. DOI: 10.1111/1750-3841.13950.
- 59. O. M. Abel, S. Chinelo, and R. Chidioka, "Enhancing cassava peels starch as feedstock for biodegradable plastic," *J Mater Environ Sci*, vol. 12, no. 2, pp. 169-182, 2021.
- 60. J. Songok, P. Salminen, and M. Toivakka, "Temperature effects on dynamic water absorption into paper," *Journal of Colloid and Interface Science*, vol. 418, pp. 373-377, 2014. DOI: 10.1016/j.jcis.2013.12.003.
- 61. K. Olonisakin, R. Li, S. He, W. Aishi, F. Lifei, C. Mengting, et al., "Flame rating of nano clay/MCC/PLA composites with both reinforced strength and toughness," *Journal of Polymer Research*, vol. 29, no. 12, 2022. DOI: 10.1007/s10965-022-03110-1.
- 62. G. Lupidi, G. Pastore, E. Marcantoni, and S. Gabrielli, "Recent Developments in Chemical Derivatization of Microcrystalline Cellulose (MCC): Pre-Treatments, Functionalization, and Applications," *Molecules*, vol. 28, no. 5, 2023. DOI: 10.3390/molecules28052009